J|A|C|S
ARTICLES
Published on Web 11/02/2004

Membrane Localization and Flexibility of a Lipidated Ras Peptide Studied by Molecular Dynamics Simulations

Alemayehu A. Gorfe, Riccardo Pellarin, and Amedeo Caflisch*

Contribution from the Department of Biochemistry, University of Zurich, Winterthurerstrasse 190, CH-8057 Zurich, Switzerland

Received June 9, 2004; E-mail: caflisch@bioc.unizh.ch

Abstract: Lipid-modified membrane-binding proteins are essential in signal transduction events of the cell, a typical example being the GTPase ras. Recently, membrane binding of a doubly lipid-modified heptapeptide from the C-terminus of the human N-ras protein was studied by spectroscopic techniques.[14] It was found that membrane binding is mainly due to lipid chain insertion, but it is also favored by interactions between apolar side chains and the hydrophobic region of the membrane. Here, 10 explicit solvent molecular dynamics simulations for a total time of about 150 ns are used to investigate the atomic details of the peptide−membrane association. The 16:0 peptide lipid chains are more mobile than the 14:0 phospholipid chains, which is in agreement with ^{2}H NMR experiments. Peptide−lipid and peptide−solvent interactions, backbone and side-chain distributions, as well as the effects of lipidated peptide insertion onto the structure, and dynamics of a 1,2-dimyristoylglycero-3-phosphocholine bilayer are described. The simulation results validate the structural model proposed by the analysis of spectroscopic data and highlight the main aspects of the insertion mechanism. The peptide in the membrane is rather rigid over the simulation time scale of about 10 ns, but different partially extended conformations devoid of backbone hydrogen bonds are observed in different trajectories.

Introduction

The regulation of cellular functions is coordinated by signal molecules. External signals transmitted across membranes and received by cellular receptors are relayed to their target by intracellular signal cascades. Posttranslational lipid-modified proteins[1,2] are commonly involved in regulation of the signal transmission processes.[3−5] Typical among fatty-acid-modified proteins is the GTPase ras. The ras signal transduction cascade is central in cell proliferation and differentiation events, in which ras proteins, by activating downstream effectors,[6,7] mediate the signal flow from receptor tyrosine kinase to the cell nucleus. Malfunction in the regulatory action (the switching function) of ras proteins leads to uncontrolled cell growth, or cancer, manifested by the fact that about one-third of all human cancers carry a mutated form of ras proteins. Detailed characterization of the molecular interactions playing a role in the ras signal transmission pathways is therefore of great importance.

The specific attachment of lipids to proteins that contain the C-terminal motif, CAAX, by cleavage and addition to the SH group of Cys, is a common structural feature in membrane proteins involved in signal transduction events. Lipidated proteins (and their analogue peptides) achieve strong binding by inserting their lipid chains into the hydrophobic core of the membrane. Thus, the major membrane-binding energy contribution comes from the hydrophobic interaction between the hydrocarbon tails of the protein and the membrane. For a maximum binding potential, ras proteins can acquire two different types of lipid modification, single or double lipid modification. Typically, ras proteins with single lipid modification also contain cluster(s) of basic amino acids and bind to negatively charged plasma membranes. The interaction between the phospholipid headgroups (of the negatively charged membranes) and the positive peptide charges provides additional attractive electrostatic energy for a stable membrane association (e.g., the K-ras protein[8]). H- and N-ras proteins require double modifications.[9] Farnesylated, but nonpalmitoylated, H- and N-ras proteins mislocate to the cytosol and break the signal cascade.[10−12] The human N-ras protein, the focus of this paper, undergoes farnesylation at the C-terminal recognition region (Cys186) followed by palmitoylation at Cys181. Single lipid modification of N-ras provides insufficient hydrophobic binding energy for it to permanently anchor to plasma membranes. As a result, a fast equilibrium between adsorbed and desorbed states is observed.

(1) Hancock, J. F.; Cadwallader, K.; Paterson, H.; Marshall, C. J. *EMBO J.* **1991**, *10*, 4033−4039.
(2) Hancock, J. F.; Paterson, H.; Marshall, C. J. *Cell* **1990**, *63*, 133−139.
(3) Reuther, G. W.; Der, C. J. *Curr. Opin. Cell Biol.* **2000**, *12*, 157−165.
(4) Miggin, S. M.; Lawler, O. A.; Kinsella, B. T. *J. Biol. Chem.* **2003**, *278*, 6947−6958.
(5) Clarke, S. *Annu. Rev. Biochem.* **1992**, *61*, 355−386.
(6) Scheffzek, K.; Ahmadian, M. R.; Kabsch, W.; Wiesmuller, L.; Lautwein, A.; Schmitz, F.; Wittinghofer, A. *Science* **1997**, *277*, 333−338.
(7) Boguski, M. S.; McCormick, F. *Nature* **1993**, *366*, 643−654.
(8) Ghomashchi, F.; Zhang, X.; Liu, L.; Gelb, M. H. *Biochemistry* **1995**, *34*, 11910−11918.
(9) Silvius, J. R. Lipidated Peptides as Tools for Understanding the Membrane Interactions of Lipid-Modified Proteins. In *Peptide Lipid*; Simon, S. A., McIntosh, T. J., Eds.; Elsevier: New York, 2002; pp 371−395.
(10) Peters, C.; Wagner, M.; Volkert, M.; Waldmann, H. *Naturwissenschaften* **2002**, *89*, 381−390.
(11) Dudler, T.; Gelb, M. H. *J. Biol. Chem.* **1996**, *271*, 11541−11547.

10.1021/ja046607n CCC: $27.50

Unlike integral proteins that are permanently anchored to membranes, the association of ras proteins to plasma membranes is an equilibrium process.[13] Because interactions with other downstream effectors occur at the membrane surface, ras proteins are functional only in the membrane-associated state and are inactive desorbed into the cytosol. Experimental studies on membrane interactions of lipid-modified proteins, mainly using lipidated peptides and artificial membranes,[9,13] have shed light on how their distribution is regulated between the active (membrane-bound) and inactive (unbound) states, as well as on the energetics and thermodynamics of the interaction.

Using a combination of Fourier transform infrared, solid-state NMR, and neutron diffraction spectroscopy, Huster et al. recently studied membrane insertion and localization of a heptapeptide representing the carboxy terminus (residues 180−186) of the human N-ras protein.[14] The plasma membrane was modeled by 1,2-dimyristoylglycero-3-phosphocholine (DMPC). This study highlighted the key structural features that accompany membrane insertion of ras proteins. The peptide inserts its two lipid chains deep into the membrane interior, such that stabilizing hydrophobic contacts between the DMPC and peptide lipid chains are possible. Binding is further assisted by the insertion of two hydrophobic amino acid side chains (Leu and Met) into the hydrophobic section of the membrane. The backbone adopts a disordered conformation and is preferentially localized in the lipid−water interface. These observations led to a plausible structural model for membrane binding of N-ras proteins.

It is worth noting that while the structure of the soluble part of ras proteins (residues 1−166) has been solved by both X-ray diffraction[15−18] and solution NMR spectroscopy,[19] there are no structural data for the C-terminal membrane binding region (residues 180−186). The biophysically derived structural model of Huster et al. for a doubly lipid-modified synthetic heptapeptide bound to a DMPC bilayer mimics the binding mode of the human N-ras protein. It is therefore of general significance. However, not all of the details of association can be observed spectroscopically; atomic level analysis of peptide−lipid and peptide−solvent interactions, backbone and side-chain distributions, as well as the effect of lipidated-peptide insertion onto the structure, and dynamics of a DMPC bilayer are required for a molecular-level interpretation and full description of the association process. A more-direct approach to investigate these and related issues is provided by computational methods. Due to the level of details that they can provide, molecular dynamics (MD) simulations of the lipidated peptide and DMPC bilayer are uniquely suited to address these questions at the atomic level.

Several explicit water MD studies of membrane−protein systems have been conducted (see, for example, review articles[20−22] and recent reports[23−25]). The majority of these simulations targeted the stability, dynamics, and functional aspects of integral proteins in a variety of membranes,[26−32] pure membranes and their environments,[33−35] and peptide−bilayer systems.[36−40] So far, however, only few attempts have been made to simulate membrane localization, and the accompanying mechanisms of insertion of peptides/proteins whose initial positions, with respect to the phospholipids, are not clearly known a priori.[41−43] Kaznessis et al. investigated the interaction between the N-terminal region of the human surfactant protein-B in dipalmitoylphosphatidylcholine (DPPC) and dipalmitoylphosphatidylglycerol (DPPG) monolayers.[41] Their simulations revealed that the peptide fragment of protein-B adopts different modes and energetics of interactions with the different phospholipid monolayers, with preferential affinity for anionic phospholipids. Knecht and Grubmüller used MD and annealing simulations to study mechanical coupling by the membrane fusion SNARE protein syntaxin 1A.[42] Their simulation results indicate that partially unstructured linkers provide significant mechanical coupling. Sankararamakrishnan and Weinstein simulated the helical region of dynorphin in a DMPC bilayer.[43] They showed that in the complex, the tilt angle of the dynorphin helix from the bilayer normal is stabilized at ∼50° for different initial orientations of the dynorphin.[43] In a recent study on the insertion of antimicrobial peptides into a zwitterionic lipid bilayer in which the peptides were directed toward the interface either on their hydrophobic or positively charged face, it was found that the former bind to the interface and subsequently penetrate the bilayer while the latter displayed only partial surface binding.[44]

In the present study, MD simulations are used to investigate the position, orientation, and flexibility of a lipidated ras peptide

(12) Nägele, E.; Schelhaas, M.; Kunder, N.; Waldmann, H. *J. Am. Chem. Soc.* **1998**, *120*, 6889−6902.
(13) Hinterding, K.; Alonso-Diaz, D.; Waldmann, H. *Angew. Chem., Int. Ed.* **1998**, *37*, 688−749.
(14) Huster, D.; Vogel, A.; Katzeka, C.; Sheidt, H. A.; Binder, H.; Dante, S.; Gutberlet, T.; Schoernig, O.; Waldmann, H.; Arnold, K. *J. Am. Chem. Soc.* **2003**, *125*, 4070−4079.
(15) Pai, E. F.; Kabsch, W.; Krengel, U.; Holmes, K. C.; John, J.; Wittinghofer, A. *Nature* **1989**, *341*, 209−214.
(16) Milburn, M. V.; Tong, L.; deVos, A. M.; Brunger, A.; Yamaizumi, Z.; Nishimura, S.; Kim, S. H. *Science* **1990**, *247*, 939−945.
(17) Brunger, A. T.; Milburn, M. V.; Tong, L.; deVos, A. M.; Jancarik, J.; Yamaizumi, Z.; Nishimura, S.; Ohtsuka, E.; Kim, S. H. *Proc. Natl. Acad. Sci. U.S.A.* **1990**, *87*, 4849−4853.
(18) Krengel, U.; Schlichting, L.; Scherer, A.; Schumann, R.; Frech, M.; John, J.; Kabsch, W.; Pai, E. F.; Wittinghofer, A. *Cell* **1990**, *62*, 539−548.
(19) Kraulis, P. J.; Domaille, P. J.; Campbell-Burk, S. L.; Akenn, T. V.; Laue, E. D. *Biochemistry* **1994**, *33*, 3515−3531.
(20) Pastor, R. W.; Venable, R. M.; Feller, S. E. *Acc. Chem. Res.* **2002**, *35*, 438−446.
(21) Faraldo-Gomez, J. D.; Smith, G. R.; Sansom, M. S. *Eur. Biophys. J.* **2002**, *31*, 217−227.
(22) Liang, J. *Curr. Opin. Chem. Biol.* **2002**, *6*, 878−884.
(23) Aksimentiev, A.; Balabin, I. A.; Fillingame, R. H.; Schulten, K. *Biophys. J.* **2004**, *86*, 1332−1344.
(24) Allen, T. W.; Andersen, O. S.; Roux, B. *Proc. Natl. Acad. Sci. U.S.A.* **2004**, *101*, 117−122.
(25) Gao, M.; Craig, D.; Lequin, O.; Campbell, I. D.; Vogel, V.; Schulten, K. *Proc. Natl. Acad. Sci. U.S.A.* **2003**, *100*, 14784−14789.
(26) Domene, C.; Bond, P. J.; Sansom, M. S. *Adv. Protein Chem.* **2003**, *66*, 159−193.
(27) Saiz, L.; Bandyopadhyay, S.; Klein, M. L. *Biosci. Rep.* **2002**, *22*, 151−173.
(28) Sansom, M. S.; Shrivastava, I. H.; Bright, J. N.; Tate, J.; Capener, C. E.; Biggin, P. C. *Biochim. Biophys. Acta* **2002**, *1565*, 294−307.
(29) Chung, S. H.; Kuyucak, S. *Biochim. Biophys. Acta* **2002**, *1565*, 267−286.
(30) Hansson, T.; Oostenbrink, C.; van Gunsteren, W. *Curr. Opin. Struct. Biol.* **2002**, *12*, 190−196.
(31) Sansom, M. S.; Bond, P.; Beckstein, O.; Biggin, P. C.; Faraldo-Gomez, J.; Law, R. J.; Patargias, G.; Tieleman, D. P. *Novartis Found. Symp.* **2002**, *245*, 66−78; discussion 79−83, 165−168.
(32) Roux, B. *Acc. Chem. Res.* **2002**, *35*, 366−375.
(33) Róg, T.; Pasenkiewicz-Gierula, M. *Biophys. J.* **2002**, *81*, 2190−2202.
(34) Böckmann, R. A.; Grubmüller, H. *Angew. Chem., Int. Ed.* **2004**, *43*, 1021−1024.
(35) Böckmann, R. A.; Hac, A.; Heimburg, T.; Grubmüller, H. *Biophys. J.* **2003**, *85*, 1647−1655.
(36) La Rocca, P.; Biggin, P. C.; Tieleman, D. P.; Sansom, M. S. *Biochim. Biophys. Acta* **1999**, *1462*, 185−200.
(37) Aliste, M. P.; MacCallum, J. L.; Tieleman, D. P. *Biochemistry* **2003**, *42*, 8976−8987.
(38) Law, R. J.; Tieleman, D. P.; Sansom, M. S. *Biophys. J.* **2003**, *84*, 14−27.
(39) Tarek, M.; Maigret, B.; Chipot, C. *Biophys. J.* **2003**, *85*, 2287−2298.
(40) Tieleman, D. P.; Sansom, M. S.; Berendsen, H. J. *Biophys. J.* **1999**, *76*, 40−49.
(41) Kaznessis, Y. N.; Kim, S.; Larson, R. G. *J. Mol. Biol.* **2002**, *322*, 569−582.
(42) Knecht, V.; Grubmüller, H. *Biophys. J.* **2003**, *84*, 1527−1547.
(43) Sankararamakrishnan, R.; Weinstein, H. *Biophys. J.* **2000**, *79*, 2331−2344.
(44) Shepherd, C. M.; Vogel, H. J.; Tieleman, D. P. *Biochem. J.* **2003**, *370*, 233−243.

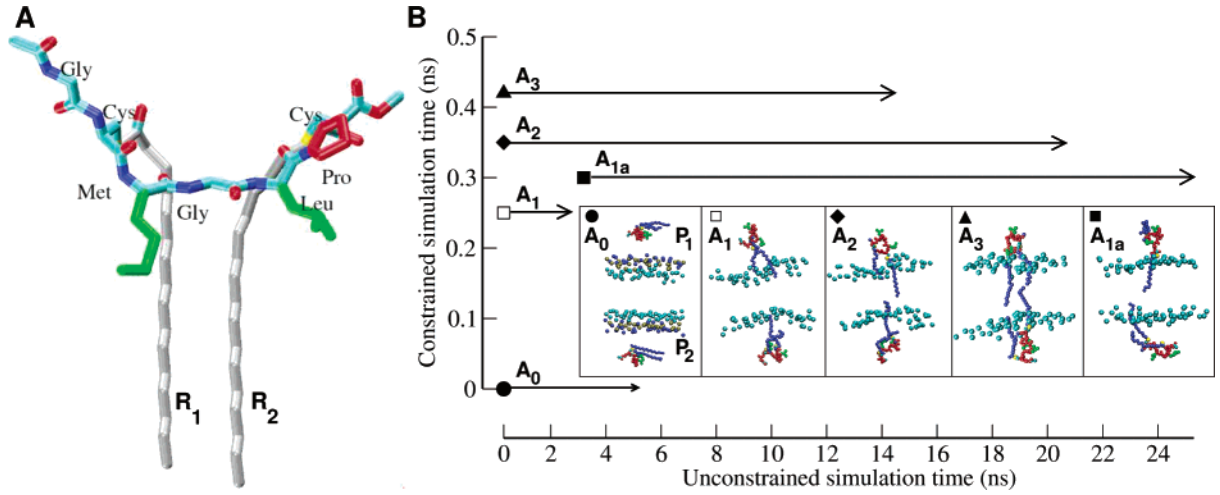

Figure 1. (A) Sequence and starting structure of the acetylated form of the N-ras peptide used in the simulations. The structure is modeled as described in the text. (B) Schematic picture of the approach used to determine initial peptide positions with respect to the bilayer. After construction of the bilayer−water system (see text), one peptide was placed in the middle of the water slabs at each monolayer. The system was relaxed for 0.25 ns. Then, one simulation was continued without any bias (A_0), while in another simulation, the separation along the membrane normal between the methyl carbon atoms of the ras lipids [C_{16}, $R_1(P_1)$ and C_{16}, $R_1(P_2)$; and C_{16}, $R_2(P_1)$ and C_{16}, $R_2(P_2)$] was decremented by 0.5 Å every 5 ps using a harmonic potential with a force constant of 100 kcal mol^{-1} Å^{-2}. The constraint was removed after 0.25 ns (starting structure for A_1), 0.35 ns (A_2), and 0.42 ns (A_3). Since P_2 and P_1 in trajectories A_1 and C_1 have completely dissociated to solvent (see Results and Discussion), the last snapshots of these were used to start trajectories A_{1a} and C_{1a}, respectively. This was done by "pulling-back-in" one chain of the dissociated peptide into the bilayer. Vertical and horizontal time axes indicate the length of the simulations with and without a harmonic constraint, respectively. The five insets show the peptide positions and orientations used as starting structures for production runs. Ras lipid chains are in blue; backbone and residue prolines are in red, while Leu and Met are in green. For clarity, only selected atoms of the DMPC are shown: phosphorus and choline nitrogen atoms in dark yellow and blue, respectively, and the first methylene carbon of the lipid tails in cyan. A similar approach was followed to obtain initial positions for simulations with a charged N-terminus.

Table 1. Performed Simulations[a]

	Acetylated N-Terminus					Charged N-Terminus				
name	A_0	A_1	A_2	A_3	A_{1a}	C_0	C_1	C_2	C_3	C_{1a}
constrained dynamics (ns)	0.0	0.25	0.35	0.42	0.10[b]	0.0	0.35	0.40	0.45	0.10[b]
unconstrained dynamics (ns)	5.0	2.3	20.1	14.1	22.5	5.0	2.6	22.3	14.2	20.0

[a] See Figure 1B for details. [b] Simulations were continued from simulations A_1 and C_1, and the constraints were applied on a single lipid chain (see text).

in a DMPC bilayer. The simulation results are first validated by comparison with NMR, Fourier transform infrared, and neutron diffraction spectroscopy experiments.[14] The good agreement between simulation and experimental results allows the use of the former to extract a clear and detailed picture of membrane insertion of the lipidated ras peptide.

Methods

It was shown experimentally that equilibrium membrane adsorption of doubly lipid-modified ras peptides have average half-life times in the order of hours to days.[45,46] Although it would be interesting to simulate the system long enough for the peptide to insert spontaneously, this is impossible to achieve within the current accessible time scales of MD simulations. A procedure to speed up the insertion is therefore necessary. The initial position and orientation of the peptide with respect to the bilayer were chosen such that insertion could be observed within a reasonable simulation time. Furthermore, to maximize sampling, two peptides (i.e., one peptide per leaflet) were simulated in each MD run. This is partly justified by the fact that the lipid bilayers are symmetrical in a simulation box and also because, in the in vitro experiments, the two leaflets were both populated.

Peptide Structure. The peptide sequence used in the simulations consisted of residues (X)Gly-Cys(R_1)-Met-Gly-Leu-Pro-Cys(R_2)-OMe, where R_1 and R_2 represent the lipid modifications (i.e., palmitic and hexadecyl thioether tail, respectively).[14] The latter was preferred to the natural occurring farnesyl to directly compare with the experimental data.[14] The X represents a hydrogen atom in the case of a charged N-terminus and an acetyl (CH_3OC-) in the neutral form of the peptide. Since the peptide sequence corresponds to the C-terminal end of the N-ras protein, the neutral form is closer to the natural protein, while the charged form corresponds to the one used in the experiments.[14] Parameters for the lipid modifications were derived from the CHARMM27 force field.[47,48] A model for the structure of the peptide was then built manually and minimized by 1000 steps SD and 1000 steps conjugate gradient to remove bad atomic contacts, leading to the structure shown in Figure 1A.

Initial Peptide Positions and Orientations. Figure 1B and Table 1 schematically show the strategy used to obtain starting structures. First, the peptides were placed in the middle of each water slab and relaxed for 0.25 ns. Then, one trajectory was continued without any bias (A_0), and another trajectory was continued with distance constraints. In the latter, the distances along the *z*-axis between corresponding C_{16} atoms of peptide 1 (P_1) and peptide 2 (P_2), i.e., $R_1(P_1)-R_1(P_2)$ and $R_2(P_1)-R_2(P_2)$, were slowly decreased by applying a harmonic force constant (see legend of Figure 1B for details). By removing the

(45) Shahinian, S.; Silvius, J. R. *Biochemistry* **1995**, *34*, 3813−3822.
(46) Schroeder, H.; Leventis, R.; Rex, S.; Schelhaas, M.; Nagele, E.; Waldmann, H.; Silvius, J. R. *Biochemistry* **1997**, *36*, 13102−13109.
(47) Feller, S. E.; Yin, D.; Pastor, R. W.; MacKerell, A. D., Jr. *Biophys. J.* **1997**, *73*, 2269−2279.
(48) MacKerell, A. D., Jr.; Bashford, D.; Bellott, M.; Dunbrack, R. L.; Evanseck, J. D.; Field, M. J.; Fischer, S.; Gao, J.; Kuchnir, L.; Guo, L.; Guo, H.; Kuczera, K.; Lau, F. T. K.; Mattos, C.; Joseph-McCarthy, D.; Michnick, S.; Ngo, T.; Nguyen, D. T.; Prodhom, B.; Reiher, W. E., III.; Roux, B.; Schlenkrich, M.; Smith, J. C.; Stone, R.; Straub, J.; Watanabe, M.; Wiorkiewicz-Kuczera, J.; Karplus, M. *J. Phys. Chem. B* **1998**, *102*, 3586−3616.

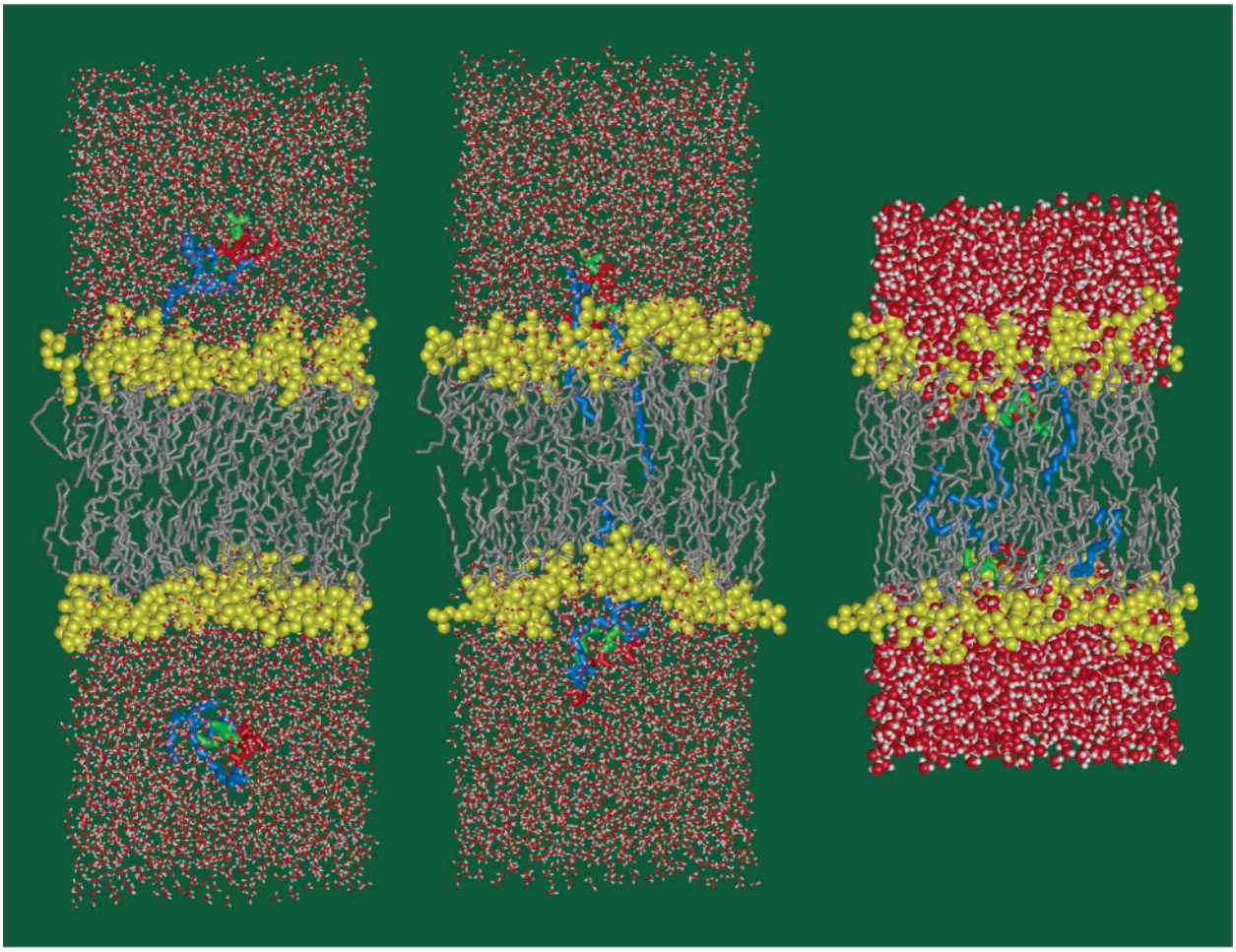

Figure 2. Snapshots after 0.25 ns of relaxation (A_0, left), after partial insertion promoted by a 0.35 ns constrained dynamics (A_2, middle), and the final snapshot (A_2, right). Backbone and Pro are in red, ras lipid chains in blue, Leu and Met side chains in green, DMPC hydrocarbon tails in gray, headgroup atoms in yellow, and water molecules in sticks (or ball-and-sticks). Part of the water molecules have been removed after partial insertion of the peptide. Hydrogen atoms of the peptide and the DMPCs are omitted for clarity.

constraint at 0.25 ns, 0.35 ns, and 0.42 ns, we obtained three starting configurations for simulations A_1, A_2, and A_3. A similar procedure was used to generate starting structures for another four trajectories calculated with a charged N-terminus (C_0−C_3). Furthermore, two trajectories, A_{1a} and C_{1a}, were started from the final conformation of simulations A_1 and C_1, respectively (see legend of Figure 1B). In total, 10 simulations were run to investigate the insertion process (Table 1).

Simulation Protocol. The CHARMM program[49] and the CHARMM27[47,48] parameters were used in all of the simulations and for part of the analysis. The construction and setup of the simulation system were based on the protocol of Woolf and Roux,[50,51] adjusted to the specificities of the present system. The liquid-crystalline phase of the DMPC (at a temperature of 310 K, the temperature at which most of the experiments were done[14]) was simulated at a constant number of particles (N), normal pressure (P_N), cross sectional area (A), and temperature (T), the NP_NAT ensemble.

To avoid strain of the bilayer due to the insertion of the two "foreign" lipid chains of the ras peptide, the cross sectional area of each monolayer was made slightly larger than that in a pure DMPC bilayer. Thus, the total lateral area per leaflet was calculated for 27 lipids with an area per lipid of 59.8 Å^2 (ref 52) to be used for 26 lipids per leaflet in all of the simulations involving peptide insertion. The peptide:DMPC ratio was therefore 1:26 in the simulations, in contrast with the experimental ratio of 1:10. Note that a more-dilute solution is preferable to make sure that multimer formation is avoided, as was also mentioned by Huster et al.. In the control simulation of a DMPC bilayer without the peptides, 27 lipids per leaflet were used within the same cross-sectional area.

The DMPC bilayer was constructed by randomly choosing structures from the pre-equilibrated phospholipid structural libraries.[53,54] To model the bulk solvent, a water slab was constructed from a pre-equilibrated TIP3 model and overlayed on the glycerol region of each leaflet. One peptide was then inserted into each of the water slabs, and water molecules closer than 2.6 Å to any peptide atom were deleted. The size of the water box was chosen such that any atom of a peptide is at least 10 Å away from the edge of the box, including the side parallel to the lipid lateral surface. The dimension of the system was 43.6 × 37.2 × 120.0 Å^3, resulting in a total of ∼4350 water molecules, 2 peptides, and 52 DMPC lipids. In the case of the simulations with a charged N-terminus, the system was neutralized by adding a chloride ion in each water box. The simulation systems for the neutral and charged peptides contained a total of 19 560 and 19 575 atoms, respectively. Figure 2 (left and middle) shows representative snapshots of the simulation setup.

(49) Brooks, B. R.; Bruccoleri, R. E.; Olafson, B. D.; States, D. T.; Swaminathan, S.; Karplus, M. *J. Comput. Chem.* **1983**, *4*, 187−217.
(50) Woolf, T. B.; Roux, B. *Proc. Natl. Acad. Sci. U.S.A.* **1994**, *91*, 11631−11635.
(51) Woolf, T. B.; Roux, B. *Proteins* **1996**, *24*, 92−114.
(52) Petrache, H. I.; Dodd, S. W.; Brown, M. F. *Biophys. J.* **2000**, *79*, 3172−3192.
(53) Venable, R. M.; Zhang, Y.; Hardy, B. J.; Pastor, R. W. *Science* **1993**, *262*, 223−226.
(54) de Loof, H. D.; Harvey, S. C.; Segrest, J. P.; Pastor, R. W. *Biochemistry* **1991**, *30*, 2099−2113.

Subsequent minimizations and a 200 ps equilibration with progressively decreasing harmonic constraints on the peptide backbone, side chains, lipid headgroups, and water oxygen atoms were similar to those of previous reports.[55] After equilibration, production simulations were run in the NP_NAT ensemble. Periodic boundary conditions in all three spatial directions were used, with constant normal pressure ($P_N = 1$ atm) and constant A and T. Constant temperature was maintained using the Hoover temperature control[56] with a thermal piston mass of 3000 kcal mol^{-1} ps^2. Truncation of electrostatic interactions has been shown to have major effects on the bilayer properties.[57] In this work, long-range electrostatic interactions were treated by the particle mesh Ewald (PME) method[58] with a 12 Å cutoff for direct and reciprocal space summations. A shift function at 10 Å for the Lennard-Jones interactions and a heuristic update of the nonbonded list, with a cutoff at 12 Å, were used. The integration time step was 2 fs, and all bonds involving hydrogens were fixed using the SHAKE algorithm. Structures were saved every 1 ps for analysis.

To speed up sampling, part of the water layer was removed after a portion of the peptides had inserted into the bilayer, while keeping sufficient waters to solvate both the peptides and the bilayer. This resulted in a reduction of 40% in the total number of atoms (Figure 2, right). In the early stages of the simulations, drift of the peptide along the lateral spatial directions (i.e., perpendicular to the membrane normal) was prevented by applying a cylindrical potential.[50] This constraint was removed after partial insertion to allow a spontaneous lateral reorganization of the peptide in the bilayer.

Analysis. The bilayer thickness (D_{PP}) is defined as the distance between the geometric center of the phosphorus atoms at each monolayer. The average chain length (L_C) is defined as the average distance along the bilayer normal between the first methylene carbon and the terminal methyl carbon atoms of the lipid chains,[59] calculated from trajectories as

$$\langle L_C \rangle \equiv \langle z_2 \rangle - \langle z_x \rangle \quad (1)$$

where x is 14 for the DMPC chains and 16 for the ras chains, and the $\langle\rangle$ denote time averages. Note that L_C, defined here, is equivalent to L^*_C in the literature,[59] which does not include the distance from the first methylene to the carbonyl carbon (~0.55 Å) and the extra length of the terminal methyl group (~0.98 Å).[59]

The deuterium order parameter, S_{CD}, was calculated as

$$S_{CD} = \frac{1}{2}\langle 3\cos^2\theta_n - 1\rangle \quad (2)$$

where θ_n is the instantaneous angle between a vector along the methylene/methyl hydrogens of the acyl carbon atoms and the bilayer normal.

Graphical analysis of the simulations was made using the VMD program.[60]

Results and Discussion

Control Simulations. To check the behavior and stability of the DMPC bilayer and the peptide alone in water, simulations with the same setup as that in the multicomponent simulations were performed for each isolated component. Furthermore, the effect on the insertion mechanism of the lipid tails was assessed by simulating the peptide without lipid tails under the same conditions as those for the lipid-modified peptide.

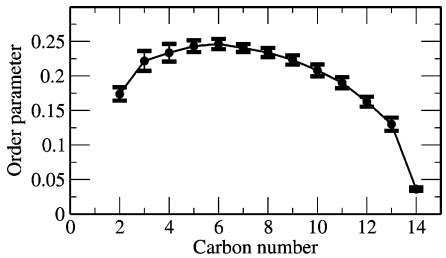

Figure 3. Deuterium order parameters of hydrocarbon tails from the 6 ns DMPC trajectory without peptides. The error bars are calculated by dividing the last 4 ns of the trajectory in segments of 1 ns.

Peptide in Water. One factor that may affect the rate of peptide insertion is its structural properties in water. To assess the behavior of the peptide in water, a short simulation of 2 ns was performed in a cubic box of TIP3 waters. As may be expected for a system with no charged or polar side chains, the peptide quickly adopted a collapsed conformation. It buried a large part of its hydrophobic surface by "sequestering" the apolar amino acids, Met and Leu, with the lipid hydrocarbon chains (data not shown). The short simulation does not allow one to describe the accessible conformational space.

DMPC in Water. A 6 ns trajectory of the DMPC bilayer was run to investigate the bilayer behavior in the absence of the peptides and to facilitate structural comparison with simulations in the presence of the ras peptide. The trajectory was stable, and the bilayer structural properties were generally the same as in previous reports.[55] The bilayer thickness (D_{PP}) is a useful parameter for estimating bilayer structural changes upon protein insertion. The average D_{PP} value calculated from the simulation without peptides (37.0 Å, see Table 4) is in good agreement with previous calculations using the same protocol (35.9 Å)[55] and is close to the experimental thickness (i.e., the average distance between lipid headgroups at each monolayer measured by electron density profile method) of 36.0 Å.[61] The deuterium order parameters (S_{CD}, eq 2), calculated from the simulation (Figure 3), are typical of other DMPC simulations[62] and in very good agreement with experimentally measured values at 30 °C.[52] Possible structural alterations after peptide insertions can therefore be safely attributed to changes arising from the insertion of the peptide.

Peptide without Lipid Tails. Three trajectories with the same starting conditions as those in trajectories A_2, A_3, and A_{1a}, but lacking the palmitoyl and hexadecyl groups, were run for 2.5 ns each. Four of the six peptides fully dissociated into water. For the remaining two peptides, most of the backbone and side chains moved toward bulk water within 2.5 ns, with only the N-terminus maintaining contact with the headgroup region of the bilayer. This suggests that lipid modifications are essential for membrane insertion.

Peptide Insertion. The location of the geometric center of the peptides and the initial number of peptide−DMPC contacts were used to monitor the insertion process and peptide−bilayer interactions. Table 2 summarizes the initial and final peptide locations, as well as the initial number of ras acyl carbon atoms in contact with those of DMPC. Initial peptide positions varied between 41 (completely in water) and 16 Å (partly inserted).

(55) Petrache, H. I.; Grossfield, A.; MacKenzie, K. R.; Engelman, D. M.; Woolf, T. B. *J. Mol. Biol.* **2000**, *302*, 727−746.
(56) Hoover, W. G. *Phys. Rev. A* **1985**, *31*, 1695−1697.
(57) Patra, M.; Karttunen, M.; Hyvonen, M. T.; Falck, E.; Lindqvist, P.; Vattulainen, I. *Biophys. J.* **2003**, *84*, 3636−3645.
(58) Darden, T.; York, D.; Pedersen, L. *J. Chem. Phys.* **1993**, *98*, 10089−10092.
(59) Petrache, H. I.; Tu, K.; Nägle, J. F. *Biophys. J.* **1999**, *76*, 2479−2487.
(60) Humphrey, W.; Dalke, A.; Schulten, K. *J. Mol. Graphics* **1996**, *14*, 33−38.
(61) Nagle, J. F.; Tristram-Nagle, S. *Biochim. Biophys. Acta* **2000**, *1469*, 159−195.
(62) Moore, P. B.; Lopez, C. F.; Klein, M. L. *Biophys. J.* **2001**, *81*, 2484−2494.

Table 2. Initial and Final Peptide Positions[a]

		A_0	A_1	A_2	A_3	A_{1a}	C_0	C_1	C_2	C_3	C_{1a}
Number of Ras Acyl Carbon Atoms in Contact with DMPC Acyl Carbons at the Start[b]											
P_1	R_1	0	**7**	**15**	**15**	**15**	0	1	**4**	**8**	**7**
	R_2	0	3	**10**	**12**	**0**	0	2	**7**	**11**	0
P_2	R_1	0	0	**0**	**6**	**0**	0	**1**	**8**	**11**	**15**
	R_2	0	4	**11**	**15**	**7**	0	**11**	**11**	**16**	**16**
Distances between Peptide Geometric Centers and the Center of Bilayer (initial → final) (Å)[c]											
P_1		39 → 39	26 → 22	**19 → 10**	**17 → 10**	**22 → 13**	41 → 44	30 → 38	**24 → 9**	**21 → 9**	24 → 23
P_2		34 → 34	28 → 33	**23 → 8**	**19 → 12**	**23 → 9**	41 → 52	**22 → 15**	**19 → 10**	**16 → 7**	**15 → 11**

[a] P_1 and P_2 represent peptides 1 and 2, respectively, whereas R_1 and R_2 represent the palmitoyl and hexadecyl lipid tails of the ras peptide, respectively. [b] Contact is present if the ras acyl carbon is within 5 Å of at least one DMPC acyl carbon. The maximum possible number is 16 (i.e., the lengths of the palmitoyl and hexadecyl chains). [c] Initial and final peptide positions are defined by the location of the peptide geometric center in the first and last snapshots of the simulations [absolute values, as measured from the bilayer center ($z = 0$), are indicated]. The initial contacts that led to insertion (i.e., to the maximum possible number) and the corresponding locations are in bold.

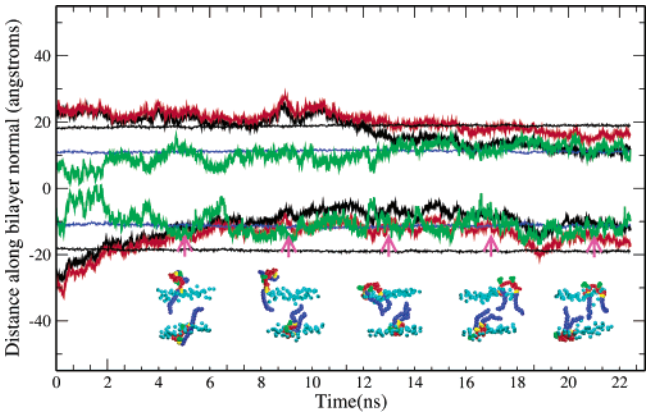

Figure 4. Time series and snapshots show the movement of the peptide toward the bilayer−water interface followed by insertion in trajectory A_{1a}. The cylindrical potential to prevent lateral motion of the peptide (see Methods) was removed at 6.5 ns. The large apparent displacement of P_1 between the snapshots at 13 and 17 ns is an effect of the periodic boundary conditions. Lines above and below $z = 0$ (the bilayer center) are for peptides 1 and 2, respectively. Thick lines: red, backbone geometric center; black, all atom geometric center; green, peptide acyl chain length. Thin lines: blue, DMPC acyl chain length; black, average phosphorus atom locations. The insets show the peptide insertion levels at selected time points during the simulations. Color codes are as in Figure 1B.

Whenever the peptide was placed near the interface with an average distance from the bilayer center of <25 Å (~7 Å from the average phosphorus atoms location), a subsequent insertion was observed (shown in bold, Table 2).

Figure 4 shows the progress of peptide insertion during the longest trajectory (A_{1a}). The peptides slowly approach the bilayer (at times even immersing in the hydrophobic region; heavy black lines) and eventually stabilize, with the backbone occupying the interfacial region. In agreement with Fourier transform infrared experiments,[14] the acyl chain lengths of the ras peptides equilibrate at lengths equivalent to those of the DMPC lipids tails, but the length fluctuations are much larger in the former. As can be seen from the insets of Figure 4, the peptide−DMPC hydrophobic contacts progressively increase along the trajectories. The two peptides move independently of each other; initially, they occupied similar locations in the middle of each monolayer but then translated to opposite corners of the monolayers' cross sectional area (inset).

Furthermore, the calculated center of mass of the peptides and the monolayers in the unconstrained simulations indicate that while the motion of the two monolayers relative to each other is negligible, there is a substantial lateral movement of each peptide independently of the other (data not shown). All of the simulations where insertions have been achieved show similar behavior. These observations indicate that once the peptides are inserted, the previous history (including the starting position and orientation) is forgotten. The mobility of the peptide at the membrane surface is qualitatively similar to that seen in a recent MD study of a membrane-anchored single-lipidated peptide.[63,64] Furthermore, the values of the two-dimensional diffusion constant on the membrane plane computed from the trajectories,[35] $\sim 10-30 \times 10^{-8}$ cm^2 s^{-1} for the DMPC and $\sim 6-15 \times 10^{-8}$ cm^2 s^{-1} for the peptide, suggest that the peptide moves slightly slower than individual lipids. The diffusion of the DMPC lipids is within the range of excimer experiments.[65]

Comparison of the trajectories, based on the contact criteria, may give a more-detailed picture of the insertion process. Although insertion was not observed in the simulations where no initial peptide−DMPC contacts were present (A_0 and C_0), a minimum of roughly 5−7 inserted carbon atoms per acyl chain is sufficient to spontaneously lead to full insertion. A smaller number of ras acyl carbons contacting DMPC acyl carbons did not result in insertion within the time scale of the simulations. For example, while seven carbon−carbon contacts between ras and the DMPC lipids resulted in insertion (e.g., P_2 in A_{1a} and in C_{1a}), three or four contacts could not stabilize the ras peptide in the bilayer and led to desorption to water (P_2 in A_1 and P_1 in C_1). Interestingly, even a chain with no or few initial contacts subsequently inserts if the other chain is involved in a sufficient number of initial contacts with the bilayer (e.g., P_2 in A_2 and in C_1). As an example in trajectory A_2, the palmitic chain (R_1) of P_2 was in water at the start and early stages of the simulation; its insertion began at about 9.3 ns, and after fluctuating for about 2 ns, it made a stable association from 11 ns onwards (Figure 5). In total, five cases of single chain preinsertion were used to investigate the behavior of the complex where only a single chain of a peptide was initially in contact with the bilayer [A_{1a}, $R_1(P_2)$ and $R_2(P_1)$; A_2, $R_1(P_2)$; C_1, $R_1(P_2)$; C_{1a}, $R_2(P_1)$]. It was anticipated that the palmitoyl chain R_1 (in trajectories A_{1a}, A_2, and C_1) and the hexadecyl chain R_2 (in trajectories A_{1a} and C_{1a}) would insert spontaneously. A total of three and one spontaneous insertions of the palmitoyl and hexadecyl chains were observed, respectively, whereas the hexadecyl group did not insert in the 20 ns simulation of C_{1a} (Table 3). Despite the limited statistics, it appears that there is no significant difference in the times

(63) Nagle, J. F. *Biophys. J.* **1993**, *64*, 1476−1481.
(64) Jensen, M. O.; Mouritsen, O. G.; Peters, G. H. *Biophys. J.* **2004**, *86*, 3556−3575.
(65) Blume, A. Dynamic Properties. In *Phospholipid Handbook*; Cevc, G., Ed.; Marcel Dekker: New York, 1993; pp 455−552.

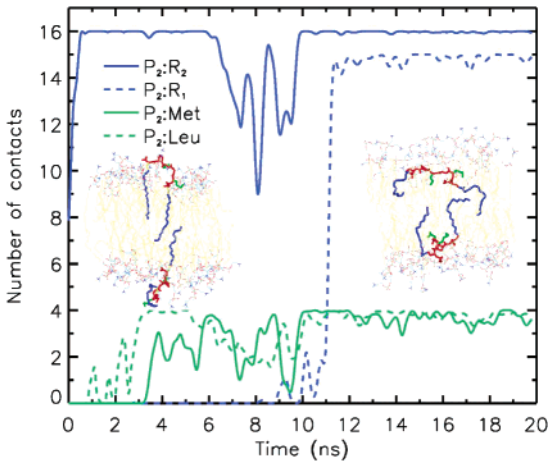

Figure 5. Peptide−DMPC hydrophobic interactions along trajectory A_2. Interactions are defined as the number of ras methylene/methyl carbons and Leu and Met side chain heavy atoms, within 5 Å of DMPC methylene/methyl carbons. For clarity, the data shown are only for peptide 2. The insets represent the system before (left, at 2 ns) and after (right, at 20 ns) complete insertion of peptide 2 (shown in the lower leaflet of the insets). The hydrophobic groups of ras interacting with the DMPC hydrophobic core are colored in blue and green; the DMPC lipid tails are in yellow, and the headgroups are in "standard" atom colors.

Table 3. Approximate Insertion Times (in nanoseconds) of Palmitoyl and Hexadecyl Groups of the Peptide[a]

chain (peptide)	time	trajectory
$R_1(P_2)$	2.4 (0.0)	C_1
$R_1(P_2)$	11.3 (9.3)	A_2
$R_1(P_2)$	7.0 (1.5)	A_{1a}
$R_2(P_1)$	12.3 (11.9)	A_{1a}

[a] Insertion times are measured for the insertion (distance of <5 Å from any DMPC acyl carbon) of at least 8 of the 16 ras acyl carbons. Time points where initial fluctuating contacts were made are shown in parentheses.

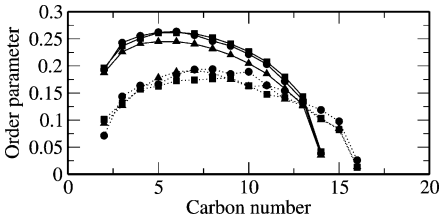

Figure 6. Deuterium order parameters of hydrocarbon tails for DMPC (solid lines) and peptide lipids (dotted lines) after insertion of the ras peptide. Circles, boxes, and triangles are for simulations C_2, A_2, and A_3, respectively.

needed for the Cys181 palmitoyl or Cys186 hexadecyl groups' spontaneous insertion. Moreover, as mentioned above, a limited preinsertion of one or both of the chains is sufficient to trigger insertion and stabilization of the whole peptide.

Lipid Bilayer Structure. Lower order parameters were observed for the 16:0 ras chains compared with the 14:0 DMPC chains.[14] The order parameters from the last 10 ns of some of the simulations that resulted in peptide insertion are shown in Figure 6. It is clear from the figure that the peptide lipid chains are significantly less ordered compared with the DMPC chains, which is in very good agreement with experiments.[14] The difference in the calculated average order parameters between the DMPC chains and the ras chains is 0.060, compared with the experimental value of 0.057. The effective length of saturated hydrocarbon chains is proportional to the average order parameters.[63] The results show that the longer 16:0 ras chains decrease their order upon membrane insertion to match the length of the shorter 14:0 DMPC lipids. In fact, the lengths of the ras and DMPC chains become close to each other after the stabilization of the peptide in the host lipids (Figure 4).

Table 4 compares the D_{PP} values calculated for the free DMPC simulation with those of the "insertion" simulations. In all of the insertion simulations, the global thickness of the bilayer has increased by about 1 Å: an average of 38.1 Å in the presence of the peptide, compared with 37 Å for a pure DMPC simulation. This is consistent with several ^{2}H NMR and ESR experiments which showed that hydrophobic peptides increase bilayer thickness due to hydrophobic mismatch.[66] Observed globally, therefore, the structure of the bilayer is slightly perturbed by the insertion of the peptide. However, the average chain lengths (L_C, eq 1) in simulations with and without peptides are similar (Table 4).

Besides the average thickness, the local effect of the peptide on the lipid bilayer is of special interest. The average distance, D_P, of the P atoms from the bilayer center (at $z = 0$) was calculated for those P atoms that are close to the peptide (a cutoff of 8 Å) and compared with the average distance for the rest of the P atoms. In all of the simulations with insertions, the D_P in the vicinity of the peptide is decreased with respect to the average value (Table 4). In contrast, the rest of the bilayer responds by increasing its D_P. Petrache et al. observed that the bilayer thickness around the monomeric form of glycophorine A decreases, as in the ras peptide (Table 4), while an increase was observed in the dimer.[55] The change of the bilayer structure due to the insertion of peptides is a complex process involving both the length and the tilt of the peptide and the lipid.[67] The above observation therefore requires a further investigation beyond the scope of this paper.

Peptide Structure. Structural analysis of the peptide backbone, in terms of its fluctuations, presence of hydrogen bonds, and other observables, revealed that the peptide does not assume a regular secondary structure before or after membrane insertion. No backbone hydrogen bonds were observed in the simulations. The root-mean-square fluctuations (RMSF) of the C_α atoms after complete insertion (0.5−1 Å for the last 2 ns of the simulations) suggest that the peptide is rather rigid (see the thickness of the tubes in Figure 7). The peptide backbone is extended, and several conformations are observed. Furthermore, while the overall backbone and side chain membrane localization of the peptide is similar among the trajectories, cluster and principal component analyses indicate that each trajectory samples a rather different region of conformational space with few overlaps (data not shown). Comparison of the peptide structures averaged over the last 2 ns in terms of root-mean-square deviations (RMSD) also shows the same behavior (Table 5). Although the simulation times may be insufficient to allow conformational interconversion, these results indicate that a unique peptide structure may not be required for bilayer adsorption. The lack of a well-defined three-dimensional structure may be biologically relevant since it increases the likelihood of productive encounters between the peptide/protein and plasma membrane.[69,70] However, the orientation of each side chain is important for the binding, and the backbone conformation should accommodate this requirement. Figure 7 (bottom left) shows the conformational change

(66) de Planque, M. R.; Greathouse, D. V.; Koeppe, R. E., II.; Schafer, H.; Marsh, D.; Killian, J. A. *Biochemistry* **1998**, *37*, 9333−9345.
(67) Petrache, H. I.; Killian, J. A.; Koeppe, R. E.; Woolf, T. B. *Biophys. J.* **2000**, *78*, 324A.

Table 4. Structural Properties of the DMPC Bilayer[a]

	without peptides	A_2	A_3	C_2	C_3
D_{PP}	37.0 ± 0.4	38.0 ± 0.4	38.1 ± 0.3	38.1 ± 0.3	38.3 ± 0.3
L_C	11.3 ± 0.2	11.4 ± 0.2	11.2 ± 0.2	11.5 ± 0.2	11.6 ± 0.2
D_P (bound, leaflet 1)		18.2 ± 0.8	18.5 ± 0.7	17.6 ± 1.1	17.8 ± 0.8
D_P (rest, leaflet 1)		19.3 ± 0.3	19.8 ± 0.3	19.6 ± 0.2	19.4 ± 0.3
D_P (bound, leaflet 2)		17.5 ± 0.8	18.3 ± 1.0	17.9 ± 0.8	16.7 ± 0.7
D_P (rest, leaflet 2)		19.4 ± 0.3	18.6 ± 0.3	18.9 ± 0.3	19.8 ± 0.3

[a] Data are averages over the last 4 ns of each trajectory (±, standard deviations). The bilayer thickness (D_{PP}) is the distance of the average P atom locations at each monolayer. D_P is the distance of the average P atom location of a monolayer from the bilayer center, calculated for all of the P atoms, closer by at least 8 Å to any peptide heavy atom (bound), and for the remaining P atoms (rest). The D_P values are given for leaflets 1 and 2 since the level of peptide insertion at each leaflet may differ. All values are given in angstroms.

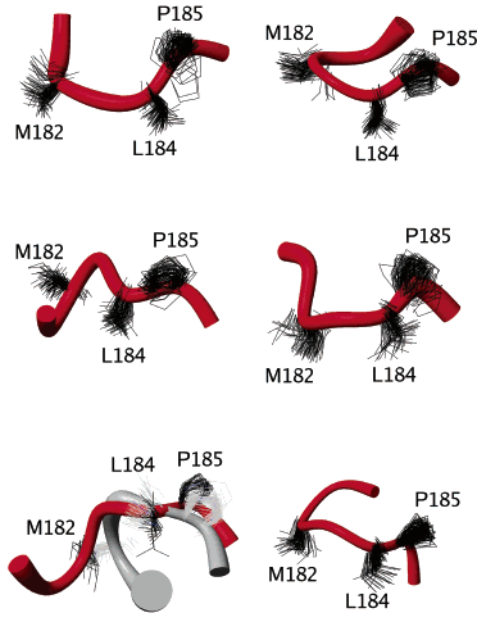

Figure 7. Average backbone structures of the peptides during the last 10 ns of trajectories A_{1a} (top), A_2 (middle), and A_3 (bottom); peptide 1 is shown in the left-hand-side and peptide 2 in the right-hand-side. The thickness of the tubes represents the root-mean-square fluctuations of the backbone. Also shown are the side chains: from left to right, Met182, Leu184, and Pro185. The bottom left structure shows the average structures before (gray) and after (red for the backbone and black for side chains) the conformational transition (see text for details). Figure made with MOLMOL.[68]

Table 5. C_α RMSD Values of the Peptide Structures in Different Insertion Simulations (angstroms)[a]

	A_2:P_1	A_2:P_2	A_3:P_1	A_3:P_2	A_{1a}:P_1	A_{1a}:P_2
A_2:P_1		2.6	1.9	3.4	2.3	3.3
A_2:P_2			3.2	2.3	1.4	2.4
A_3:P_1				4.0	2.9	4.4
A_3:P_2					2.7	1.7
A_{1a}:P_1						2.5

[a] Data for the simulations with an acetylated N-terminus are shown. The C_α RMSD values were calculated for structures averaged over the last 2 ns after complete peptide insertion.

of the backbone accompanying the rotation of the Leu side chain from water-exposed to the interior of the bilayer. Similar structural transitions are observed during the rotation and insertion of the Met side chain (data not shown). Experimentally, the amide bands in a Fourier transform infrared spectrum of the peptides at two polarizations were different, which indicates that the peptides in the sample adopt a nonrandom orientation.[14]

(68) Koradi, R.; Billeter, M.; Wuthrich, K. *J. Mol. Graphics* **1996**, *14*, 29−32, 51−55.
(69) Wright, P.; Dyson, H. *J. Mol. Biol.* **1999**, *293*, 321−331.
(70) Caflisch, A. *Trends Biotechnol.* **2003**, *21*, 423−425.

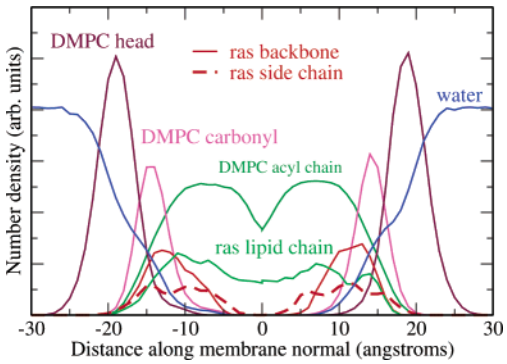

Figure 8. Number density averaged over the last 2 ns of all of the simulations that resulted in peptide insertion. Because of the different levels of peptide insertion in the earlier stages of the simulations, the average was taken in the trajectories with complete insertion and only for the last 2 ns.

Peptide Environment Interactions. Differences in the neutron scattering length density profiles between DMPC, with and without the ras peptide, were used to determine the insertion depth and distribution of the ras lipid chains as well as the distribution of backbone and side chains.[14] The ras lipid chains were found to be located in the middle of the membrane, approximately distributed within 10 Å of the bilayer center. The backbone and side chains reside in the headgroup/glycerol/upper chain region. The average number densities of the peptide lipid chains, side chains, backbone, and water, calculated from our simulations (Figure 8), strongly support these experimental findings. While the peptide lipid chains populate the interior of the bilayer and the side chains populate the upper chain region (peak at 11 Å), the backbone resides in the membrane−water interface (with a maximum at ∼13 Å) close to the DMPC carbonyl oxygens. The side chains show large variations populating the region beneath the DMPC carbonyl oxygens and the upper hydrophobic region of the bilayer. The distribution of the side chains populating the hydrocarbon region is similar to that obtained by Tieleman and colleagues for a Trp residue in their MD study of Arg/Lys containing interfacial pentapeptides partitioned in a solvated DOPC bilayer.[37] In contrast, they found that the charged Arg/Lys (as well as a Leu side chain) populates the interfacial region.

The distributions are governed by specific atomic interactions of the peptide with its environment. The carbon atoms of the ras lipid chains are in contact with carbons of the DMPC host matrix (Figures 4 and 5), contributing to stable association. In addition to the ras lipid chains, the apolar residues, Met and Leu, are involved in van der Waals interactions with the DMPC lipid chains (Figure 5). From the radial distribution functions (data not shown), polar interactions involving the amide and

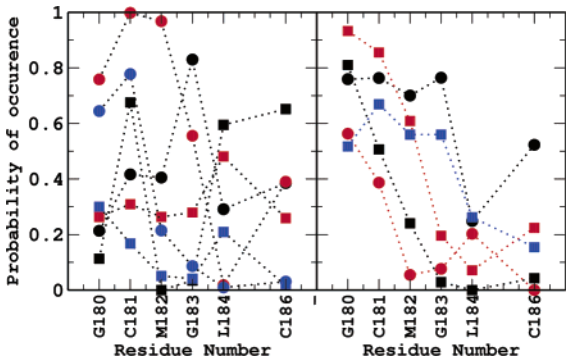

Figure 9. Probability of the occurrence of backbone amide nitrogen−phosphate oxygen hydrogen bonds in the last 10 ns of the simulations. A distance cutoff of 3.5 Å between N and O atoms was used. Left panel represents simulations with the acetylated N-terminus (A_2 in red, A_3 in black, and A_{1a} in blue). The right panel is for simulations with the charged N-terminus (C_2 in red, C_3 in black, and C_{1a} in blue). Circles are for peptide 1 and squares for peptide 2. The dotted lines are drawn only for clarity.

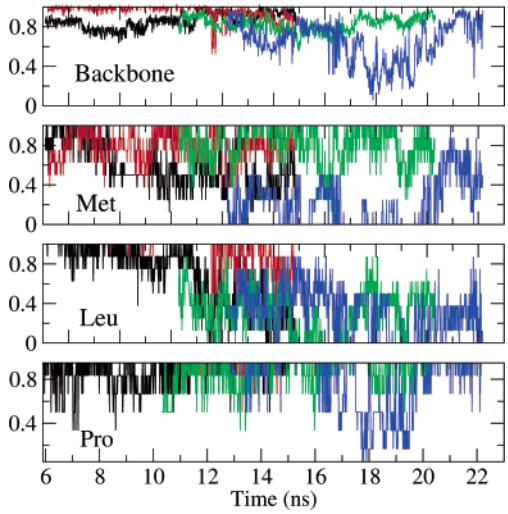

Figure 10. Number of ras atoms in contact with water during peptide insertion normalized over the number of contacts in a fully solvated extended conformation. A contact is defined as the number of ras heavy atoms within 5 Å of water oxygen atoms. The last 10 ns of A_3, C_3, A_2, and C_2 are shown in black, red, green, and blue, respectively.

carbonyl groups of the peptide backbone and the phosphate and choline groups of DMPC, respectively, anchor the peptide at the lipid−water interface. Hydrogen-bond interactions, particularly by the N-terminal side of the peptide (Figure 9), play a significant role. The plots in Figure 10 indicate the interactions of the different parts of the peptide with water in the last 10 ns of the trajectories. As expected, the Met and Leu side chains lose significant contact with water as they progressively penetrate the lipid membrane. The backbone and Pro side chain, however, remain in constant interaction with solvent. The interactions of the ras peptide with the DMPC bilayer and water are finely balanced. However, it is clear from the number of ras and DMPC acyl carbon contacts that nonpolar interactions provide the major driving force for association. The backbone and the Pro ring help maintain the location of the peptide in the interfacial region.

Peptide Stabilization in the Bilayer. Insertion of singly myristoylated or palmitoylated peptides containing positive charge clusters into bilayers with negatively charged interfaces is assisted by attractive electrostatic interactions. However, complete insertion of their lipid tails into the hydrophobic region is prevented by unfavorable electrostatic desolvation penalty.[71,72] In contrast, the completely hydrophobic polypeptide from the C-terminus of the N-ras protein was shown previously,[14] and here, to insert deep into the DMPC bilayer. This leads to a larger gain in hydrophobic stabilization compared with charged peptides. Although the insertion of the ras lipid chain is driven by hydrophobic interactions (the polar backbone−headgroup interactions playing a passive role in the initial contact formation; see the section on peptide insertion), once inserted, the backbone of the peptide contributes to the stability of the complex by interacting with the DMPC headgroups (Figure 9). Hydrogen-bonding interactions between the backbone amides (mainly involving the N-terminal segment, particularly the palmitoylated Cys181) and the phosphate oxygen atoms are frequent. The hydrogen-bonding potential appears to be slightly enhanced in the charged form of the peptide. In general, however, there was no significant difference between the charged and acetylated forms of the peptide in their interaction with the bilayer, suggesting that the hydrophobic interactions are the most crucial. This is further supported by the observed interactions between the lipid tails of the ras peptide and the DMPC. Note that the transfer from aqueous solution into a nonpolar environment of each CH2 group of lipid-modified proteins contributes about 0.8 kcal mol^{-1} of hydrophobic stabilization,[45,73] suggesting a large energetic contribution from the lipid tail interactions. Further hydrophobic stabilizations due to interactions between the apolar side chains and the DMPC hydrocarbon tails ensure a strong association.

As seen in the previous section, Met and Leu side chains orient toward the hydrocarbon core, while Pro and the backbone preferentially populate the membrane−water interface. This orientational scenario is in agreement with the experiment-based hydrophobicity scales of Wimley and White (WW scales) obtained from the partitioning of small peptides into lipid vesicles[74] and octanol.[75] The former can be interpreted as the free energy of transfer of whole peptides from water to membrane interfaces ($\Delta G_{w\to if}$) and the latter from water to the hydrocarbon (HC) core ($\Delta G_{w\to oct}$). The difference gives the relative free energy of transfer from interface to HC ($\Delta G_{if\to oct}$). When the lipid modifications are excluded, the total $\Delta G_{w\to if}$ is −0.8 kcal mol^{-1}; so, the peptide would slightly favor binding to the interface. The value of $\Delta G_{w\to oct}$ is 0.48 kcal mol^{-1}, and consequently, the free energy of interface-to-HC transfer ($\Delta G_{if\to oct}$) is 1.28 kcal mol^{-1}, such that the insertion of the nonlipid-modified peptide into the HC region would be unfavorable. The backbone is the major source of the unfavorable peptide−HC interaction as its contribution ($\Delta G^{backbone}_{if\to oct}$) is 5.6 kcal mol^{-1} (note that $\Delta G^{backbone}_{w\to if}$ and $\Delta G^{backbone}_{w\to oct}$ are 1.2 and 2.0 kcal mol^{-1} per residue, respectively[76]). However, insertion into the HC can be facilitated by side chain reorientations. When $\Delta G_{if\to oct}$ of the side chains is derived from the WW scales, Met and Leu, with −1.24 and −1.49 kcal mol^{-1}, respectively, favor

(71) Buser, C. A.; Sigal, C. T.; Resh, M. D.; McLaughlin, S. *Biochemistry* **1994**, *33*, 13093−13101.
(72) Pool, C. T.; Thompson, T. E. *Biochemistry* **1998**, *37*, 10246−10255.
(73) Peitzsch, R. M.; McLaughlin, S. *Biochemistry* **1993**, *32*, 10436−10443.
(74) Wimley, W.; White, S. *Nat. Struct. Biol.* **1996**, *3*, 842−848.
(75) Wimley, W. C.; Creamer, T. P.; White, S. H. *Biochemistry* **1996**, *35*, 5109−5124.
(76) White, S. H. *FEBS Lett.* **2003**, *555*, 116−121.

the HC region, while the two glycines, with a $\Delta G_{if\rightarrow oct}$ value of 0.68 kcal mol^{-1}, favorably interact with the interface. A Pro side chain, with −1.11 kcal mol^{-1}, would be expected to transfer to the HC, but it remains in the interface due to the rigidity of its backbone. The two Cys side chains are expected to point into the HC with a free energy gain of −1.16 kcal mol^{-1}. Any lipid modification obviously increases this value. On the basis of the WW scales, therefore, the insertion into the HC region of the apolar amino acids, as well as the interfacial localization of the backbone (as observed from the simulations), is thermodynamically favored, as is the insertion of the ras lipid tails into the HC core.

Furthermore, the insertion and stabilization of the peptide in the phospholipid required only a limited number of ras acyl carbon atoms in contact with those of DMPC (between five and seven), and insertion of one chain leads to a fast spontaneous insertion of the other. While the former confirms the hydrophobic origin of the driving force of the association, the latter may relate to the fact that singly lipid-modified peptides associate with plasma membranes with shorter half-life times.[73,77]

Conclusions

The C-terminal Cys181−palmitoyl and Cys186−farnesyl chains play a fundamental role as membrane anchors of the human N-ras protein. Recently, a battery of spectroscopic techniques was used to investigate the membrane localization of a heptapeptide with the amino acid sequence of residues 180−186 containing the two lipid modifications.[14] Here, MD simulations were used for a detailed characterization of the late stages of the insertion mechanism. The position and orientation of the ras peptide and its components (backbone, side chains, and lipid chains) during the MD runs are consistent with the spectroscopic data.[14] The agreement between simulations and experiments allows the use of the former for an atomic level description of the peptide−membrane association. The simulation results highlight four aspects that go beyond the model obtained from experiments. First, a partial insertion of both, or even only one chain, is sufficient to trigger complete insertion and stabilization of the peptide in the membrane within the time scale of the MD simulations (10−20 ns). Second, the monolayer thickness is slightly smaller for phospholipids in contact with the inserted peptide and slightly larger far away from it. Because of the simplified system used in the simulations, it is not possible to speculate if this membrane deformation is relevant for signal transduction. Third, over the 10 ns time scale of the MD simulations, the peptide backbone is rather rigid and extended, but backbone conformations differing by up to 4.0 Å are observed in different MD trajectories. It is likely that multiple peptide conformations are energetically accessible for rapid binding of the human N-ras protein to the membrane. Finally, although it is difficult to speculate on the details of the insertion mechanism (because of the constrained MD used for the initial peptide positioning), a coarse-grained sequence of events consists of an initial contact between ras lipid tails and the DMPC acyl chains, followed by complete lipid insertion, and almost concomitant side chain reorientation and backbone reorganization.

After our paper was submitted, an MD study of a synthetic, cationic C_{14}-N-acylated peptide (myristoyl−HWAHPGGHHA−amide) inserted into a dipalmitoylphosphatidylcholine (DPPC) lipid bilayer was published.[64] The force field and simulated time scale are the same as in the present work, whereas the simulation protocol (constant surface tension and only one peptide per bilayer) and phospholipids (DPPC vs DMPC) are slightly different. Interestingly, the peptide mobility at the membrane surface, as well as the multiple backbone conformations and small structural fluctuations around them, is similar in the two studies, despite the differences in peptide sequence, length, and number of lipid tails.

Acknowledgment. We gratefully acknowledge Dr. R. Böckmann for useful discussions, critical reading of the manuscript, and help in preparation of some of the figures. We thank Dr. E. Paci, G. Interlandi, and F. Rao for interesting discussions, and Dr. G. Settanni for suggesting the lipidated ras peptide as an interesting system for simulations. The simulations were performed on the Matterhorn Beowulf cluster at the Computing Center of the University of Zurich. We thank C. Bollinger and Dr. A. Godknecht for setting up the cluster, and the Canton of Zurich for generous hardware support. This work was supported by the Swiss National Competence Center in Structural Biology (NCCR).

JA046607N

(77) Silvius, J. R.; l'Heureux, F. *Biochemistry* **1994**, *33*, 3014−3022.